

Desorption Kinetics of H₂O from Cab-O-Sil-M-7D and Hi-Sil-233 Silica Particles

L.N. Dinh, M. Balooch, J.D. LeMay

January 26, 2000

U.S. Department of Energy

Lawrence
Livermore
National
Laboratory

DISCLAIMER

This document was prepared as an account of work sponsored by an agency of the United States Government. Neither the United States Government nor the University of California nor any of their employees, makes any warranty, express or implied, or assumes any legal liability or responsibility for the accuracy, completeness, or usefulness of any information, apparatus, product, or process disclosed, or represents that its use would not infringe privately owned rights. Reference herein to any specific commercial product, process, or service by trade name, trademark, manufacturer, or otherwise, does not necessarily constitute or imply its endorsement, recommendation, or favoring by the United States Government or the University of California. The views and opinions of authors expressed herein do not necessarily state or reflect those of the United States Government or the University of California, and shall not be used for advertising or product endorsement purposes.

Work performed under the auspices of the U. S. Department of Energy by the University of California Lawrence Livermore National Laboratory under Contract W-7405-Eng-48.

This report has been reproduced
directly from the best available copy.

Available to DOE and DOE contractors from the
Office of Scientific and Technical Information
P.O. Box 62, Oak Ridge, TN 37831
Prices available from (423) 576-8401
<http://apollo.osti.gov/bridge/>

Available to the public from the
National Technical Information Service
U.S. Department of Commerce
5285 Port Royal Rd.,
Springfield, VA 22161
<http://www.ntis.gov/>

OR

Lawrence Livermore National Laboratory
Technical Information Department's Digital Library
<http://www.llnl.gov/tid/Library.html>

Desorption kinetics of H₂O from Cab-O-Sil-M-7D and Hi-Sil-233 silica particles

L. N. Dinh, M. Balooch, J. D. LeMay

Chemistry and Materials Science

Lawrence Livermore National Laboratory, Livermore, CA

ABSTRACT

Temperature programmed desorption (TPD) was performed at temperatures up to 850K on Cab-O-Sil-M-7D and Hi-Sil-233 silica particles. Physisorbed water molecules on both types of silica had activation energies in the range of 9-14.5 kcal/mol. However, the activation energies of desorption for chemisorbed water varied from ~ 19 kcal/mol to > 59 kcal/mol for Cab-O-Sil-M-7D, and ~ 23-37 kcal/mol for Hi-Sil-233. Our results suggest that physisorbed water can be effectively pumped away at room temperature (or preferably at 320 K) in a matter of hours. Chemisorbed water with high activation energies of desorption (>30 kcal/mol) will not escape the silica surfaces in 100 years even at 320 K, while a significant amount of the chemisorbed water with medium activation energies (19-26 kcal/mol) will leave the silica surfaces in that time span. Most of the chemisorbed water with activation energies < 30 kcal/mol can be pumped away in a matter of days in a good vacuum environment at 500 K. We had previously measured about 0.1-0.4 wt. % of water in M9787 polysiloxane formulations containing ~ 21% Cab-O-Sil-M-7D and ~ 4% Hi-Sil-233. Comparing present results with these formulations, we conclude that absorbed H₂O and Si-OH bonds on the silica surfaces are the major contributors to water outgassing from M97 series silicones.

I. INTRODUCTION

The M97 series silicone is composed of polysiloxane gumstock (67.6 wt. %), fumed silica filler Cab-O-Sil M-7D (21.6 wt. %), precipitated silica filler Hi-Sil 233 (4 wt. %), and processing aid, chemically an ethoxy endblocked polysiloxane (6.8 wt. %). Silica occupies ~ 25.6 wt. % in these silicones, and silica surfaces are well known to have a good affinity for water adsorption. Absorbed water may play an important role on the bonding between SiO₂ particles and the silicone matrix. The outgassing of water may change the nature of the silica/silicone bonding, even possibly the mechanical behavior of the materials. It may also present a compatibility issue in scaled systems containing M97 type silicones. In a previous report,¹ we have presented data on water desorption from M9787 and M9750 (~ 50 % porosity) silicones up to 500K. In order to clearly understand the mechanism through which water is incorporated into the silicone structures and to effectively control the water content in them, we have carried out experiments on the desorption of water from Cab-O-Sil-M-7D and Hi-Sil-233 silica particles separately and up to 850K.

II. EXPERIMENTS

Small amounts (0.002-0.008 g) of pre-weighted Cab-O-Sil-M-7D or Hi-Sil-233 silica powders were enveloped in a Pt foil with a dimension of 1 cm × 1 cm. The side of the envelope facing the mass- spectrometer was perforated with many holes over the entire surface. The loaded foil was held fixed to a sample holder by ways of three mechanical

clamps and transferred into an ultrahigh vacuum (UHV) chamber with a base pressure of 10^{-6} Pa (4×10^{-7} Pa in the detector chamber) through a differentially pumped load lock. A type K thermocouple was inserted in between the Pt envelope surface and a clamp holding the envelope for temperature measurement. The samples were heated from the back sides by passing currents through a Tungsten coil located 2 mm behind the samples. The detector chamber is equipped with a quadrupole mass spectrometer (QMS) and has been described in detail elsewhere.¹

III. ANALYSIS TECHNIQUES

An approach to the extraction of the kinetic parameters from a TPD spectrum involves the plot of $\ln(-d\sigma/dt)$ vs. $1/T$ at the onset of the desorption, where σ is the surface coverage, T is the desorption temperature, and t is the desorption time. This approach has been reviewed and employed for the analysis of water desorption from M97 series silicones.¹ In this report we will also apply the variable linear ramp and iterative regression analysis techniques to extract the activation energies and pre-exponential factors of water from Cab-O-Sil-M-7D and Hi-Sil-233 silica particles. A discussion on the relative ease of use and accuracy among the three techniques will also be presented.

Variable linear ramp technique:

The rate of desorption from unit surface into vacuum can be written as:

$$-\frac{d\mathbf{s}}{dt} = \mathbf{u}\mathbf{s}^n \exp(-E_d / RT) \quad (1)$$

where n is the order of the desorption reaction, σ is ratio of surface concentration at time t over the initial surface concentration or surface coverage (dimensionless and varying from 1 to 0), ν is the pre-exponential factor (s^{-1}), E_d is the activation energy of desorption (J/mol), R is the gas constant ($8.314 \text{ J.K}^{-1}.\text{mol}^{-1}$), and T is desorption temperature in K.

In the variable linear ramp technique:

$$T = T_o + \mathbf{b} t \quad (2)$$

At peak desorption temperature T_p , and for first-order kinetics ($n=1$):

$$\frac{d\left(-\frac{d\mathbf{s}}{dt}\right)}{dT} = 0 \quad (3)$$

or

$$\frac{\mathbf{b}}{\mathbf{u}} \frac{E_d}{RT_p^2} = e^{-\frac{E_d}{RT_p}} \quad (4)$$

Equation (4) yields:

$$\ln\left(\frac{\mathbf{b}}{T_p^2}\right) = -\frac{E_d}{RT_p} + \ln\left(\frac{\mathbf{u}R}{E_d}\right) \quad (5)$$

Therefore, the activation energy of desorption E_d and the pre-exponential factor \mathbf{u} of the first H_2O desorption peak in each silica TPD spectrum (which is usually associated with physisorbed water with $n = 1$) can be obtained from the slope of the plot of $\ln(\beta/T_p^2)$ vs. $1/T_p$ and its intercept, respectively. Note that due to the presence of the $\ln(\beta/T_p^2)$ term in equation (5), an accurate extraction of kinetic parameters requires large differences in the ramp rates. With some approximations, equation (5) has also been shown to be valid for $n \neq 1$.²

Iterative regression analysis technique:

With a linear heating ramp described in equation (2), equation (1) can be rewritten as:

$$-\frac{d\mathbf{s}}{dT} = \frac{\mathbf{u}}{\mathbf{b}} \mathbf{s}^n \exp(-E_d / RT) \quad (6)$$

By integration, equation (6) becomes:

$$-\int_{s_o}^{\mathbf{s}} \frac{d\mathbf{s}}{\mathbf{s}^n} = \frac{\mathbf{u}}{\mathbf{b}} \int_0^T \exp(-\frac{E_d}{RT}) dT \quad (7)$$

or

$$\mathbf{s}^n = \left[\mathbf{s}_o^{1-n} + (n-1) \frac{\mathbf{u}}{\mathbf{b}} \int_0^T \exp(-\frac{E_d}{RT}) dT \right]^{n/(1-n)} \quad \text{for } n \neq 1 \quad (8a)$$

and

$$\mathbf{s} = \mathbf{s}_o \exp(-\frac{\mathbf{u}}{\mathbf{b}} \int_0^T \exp(-\frac{E_d}{RT}) dT) \quad \text{for } n = 1 \quad (8b)$$

K. H. Van Heek and H. Juntgen² have shown that the integral in (8a) and (8b) can be well approximated by:

$$\int_0^T \exp(-\frac{E_d}{RT}) dT \approx \frac{RT^2}{E_d} \exp(-\frac{E_d}{RT}) \quad (9)$$

Substitute $\sigma_o = 1$ and equation (9) into (8a) and (8b), equation (6) becomes:

$$-\frac{d\mathbf{s}}{dT} = \frac{\mathbf{u}}{\mathbf{b}} e^{-\frac{E_d}{RT}} \left[\mathbf{s}_o^{1-n} + (n-1) \frac{\mathbf{u}}{\mathbf{b}} \frac{RT^2}{E_d} e^{-\frac{E_d}{RT}} \right]^{n/(1-n)} \quad \text{for } n \neq 1 \quad (10a)$$

and

$$-\frac{d\mathbf{s}}{dT} = \frac{\mathbf{u}}{\mathbf{b}} \exp(-\frac{E_d}{RT} - \frac{\mathbf{u}}{\mathbf{b}} \frac{RT^2}{E_d} e^{-\frac{E_d}{RT}}) \quad \text{for } n = 1 \quad (10b)$$

With the aid of an iterative regression analysis computer program, equations (10a) and/or (10b) can be used to fit the experimental TPD spectra to obtain \mathbf{u} and E_d .

A comparison among the analysis techniques:

The main advantage of the variable linear ramp technique is that it is based on an ensemble of TPD spectra spanning a large range of β , hence it suffers less from sample to sample variation. However, this technique is time consuming and technically demanding because it requires the collection of many TPD spectra with large differences in ramping rate. The main advantage of the computer aided iterative regression analysis technique over the variable linear ramp method is that kinetic parameters can be easily obtained from a single TPD run. The main advantage of the computer aided iterative regression analysis technique over the technique based on the Arrhenius plots of $\ln(-d\sigma/dt)$ vs. $1/T$ is that the iterative regression analysis technique is much less sensitive to errors in background subtraction. E_d and u obtained from the Arrhenius plot of $\ln(-d\sigma/dt)$ vs. $1/T$ can have large errors if the slope of the Arrhenius plot is not constructed at the early onset of the desorption process where a small error in background subtraction may result in substantial errors.³ Another unique advantage of the iterative regression analysis technique is that the whole desorption curve (not just the early onset or peak-desorption temperatures) is actually used in the analysis resulting in more accurate kinetic parameters.

IV. RESULTS & DISCUSSION

Fig. 1 shows typical water TPD spectra of Cab-O-Sil-M-7D at a ramping rate of 0.44 K/s (a) and 1.64 K/s (b), and of Hi-Sil-233 at a ramping rate of 0.36 K/s (c) and 3.3 K/s (d).^{4,5} Each spectrum can be seen to consist of one desorption peak at temperature below 400 K and broader convoluted desorption peaks at higher temperatures. These peaks are

associated with physisorbed and chemisorbed water from silica surfaces.^{6,7} Note that, except for an observed shift of the desorption peaks to higher temperatures, the general features of the TPD spectra do not change with increases in the ramp rate from 0.3 to 3.3 K/s. In agreement with many recent reports on water desorption from silica, we associate the lowest desorption peaks in each spectra to physisorbed water.^{6,7} As will be shown later, physisorbed water can be effectively pumped out in a vacuum environment at room temperature while chemisorbed water cannot. This explains why the ratios of the desorption-peaks at temperatures below 450 K to the desorption-peaks at higher temperatures vary from sample to sample depending on the pumping time prior to TPD experiment as seen in Fig. 1.

The plots of $\ln(\beta/T_p^2)$ vs. $1/T_p$ for the first TPD peaks of Cab-O-Sil-M-7D and Hi-Sil-233 are shown in Fig. 2 (a) and (b). The ramp rate was varied between 0.36 K/s and 10K/s for Cab-O-Sil-M-7D and between 0.36 K/s and 8.8 K/s for Hi-Sil-233 . The activation energies and pre-exponential factors obtained from the plots are from 9 to 12 kcal/mol and from 2×10^3 to $7.3 \times 10^5 \text{ s}^{-1}$ for Cab-O-Sil-M-7D (mean values: 10.5 kcal/mol and $4.5 \times 10^4 \text{ s}^{-1}$) and from 9.5 to 14.5 kcal/mol and from 1.1×10^3 to $1.6 \times 10^8 \text{ s}^{-1}$ for Hi-Sil-233 (mean values: 12 kcal/mol and $6.0 \times 10^5 \text{ s}^{-1}$).⁸ It is noted, here, that because the rate constant ($v \cdot \exp[-E_d/RT]$) depends on E_d exponentially and on v linearly, a small variation in E_d corresponds to a much larger change in v for the same rate constant. The plots of $\ln(\beta/T_p^2)$ vs. $1/T_p$ for the second (broad) TPD peaks of Cab-O-Sil-M-7D and Hi-Sil-233 are shown in Fig. 2 (c) and (d). Due to the limitation of our heater in maintaining high ramp rates at high temperatures, the ramp rates used in constructing Fig. 2 (c) and (d) was only from 0.36 K/s to 1.64 K/s for Cab-O-Sil-M-7D and 0.36 K/s to 3.3

K/s for Hi-Sil-233. The activation energies and pre-exponential factors for these broad second TPD peaks are from 14.8 to 20.4 kcal/mol and from 2×10^4 to $4.1 \times 10^6 \text{ s}^{-1}$ for Cab-O-Sil-M-7D (mean values: 17.6 kcal/mol and $2.9 \times 10^5 \text{ s}^{-1}$) and from 19.6 to 28.9 kcal/mol and from 3.0×10^5 to $8.7 \times 10^8 \text{ s}^{-1}$ for Hi-Sil-233 (mean values: 24.2 kcal/mol and $1.6 \times 10^7 \text{ s}^{-1}$).⁸ Note that the water signals from Cab-O-Sil-M-7D remain high and flat beyond the second TPD peak and that the second TPD peaks of Hi-Sil-233 are very broad (Fig. 1). Hence, the kinetic parameters obtained from the variable linear ramp technique serve only as rough estimates for the broad second desorption peak of Hi-Sil-233 and as lower limits for the flat extended portion of the desorption spectra of Cab-O-Sil-M-7D. Later on, we will deconvolve these broad and/or extended desorption peaks into distinct desorption curves using the technique of iterative regression analysis to obtain more detailed information on the kinetic parameters associated with these peaks.

Fig. 3 shows the Arrhenius plots of $\ln(-d\sigma/dt)$ vs. $1/T$ at the onset of the TPD spectra of the Cab-O-Sil-M-7D sample with a ramp rate of 0.44 K/s and of the Hi-Sil-233 sample with a ramp rate of 3.3 K/s. Analogous plots were obtained for the Cab-O-Sil-M-7D sample with a ramp rate of 1.64 K/s and of the Hi-Sil-233 sample with a ramp rate of 0.36 K/s. The activation energies of desorption and pre-exponential factors can be obtained from the slope and the intercept of such plots.¹ Obtained values of E_d and ν are tabulated in table I.

	First desorption-peak of Cab-O-Sil-M-7D samples		First desorption-peak of Hi-Sil-233 samples	
β (K/s)	0.44	1.64	0.36	3.3
E_d (kcal/mol)	12 ± 1.3	9.2 ± 0.3	11.5 ± 1.0	15 ± 0.8
u (s^{-1})	$6.7 \times 10^4 s^{-1}$ to $3.6 \times 10^7 s^{-1}$	$1.1 \times 10^3 s^{-1}$ to $3.4 \times 10^3 s^{-1}$	$2.5 \times 10^4 s^{-1}$ to $5.8 \times 10^5 s^{-1}$	$2.6 \times 10^7 s^{-1}$ to $4.3 \times 10^8 s^{-1}$

Table I: Kinetic parameters of the first desorption-peaks of Cab-O-Sil-M-7D and Hi-Sil-233 as obtained from the plots of $\ln(-d\sigma/dt)$ vs. $1/T$.⁸

The values of E_d and u listed in this table agree with those obtained by the linear variable ramp technique. However, there are 25 % differences in values of E_d from within the two Cab-O-Sil-M-7D samples and the two Hi-Sil-233 samples. This is most probably due to the sensitivity of the slopes and intercepts of the plots of $\ln(-d\sigma/dt)$ vs. $1/T$ at the early onset of the desorption process on small errors in background subtraction.³ In order to extract the kinetic parameters of the broader desorption peaks at higher temperatures by this technique, a deconvolution is needed. So, the iterative regression analysis technique

has an added advantage over the technique based on the Arrhenius plot of $\ln(-d\sigma/dt)$ vs. $1/T$ and the linear variable ramp technique, since one can simultaneously obtain E_d and ν while deconvolving the peaks.

Since the TPD spectra presented in Fig. 1 are typical of desorption processes in Cab-O-Sil-M-7D and Hi-sil-233 at different ramp rates, it is, therefore, sufficient to derive the kinetic parameters of Cab-O-Sil-M-7D and Hi-Sil-233 by the technique of iterative regression analysis from the TPD spectra that span the broadest temperature range possible. Based on this criterion, we chose to analyze the Cab-O-Sil-M-7D sample with a ramp rate of 0.44 K/s and the Hi-Sil-233 sample with a ramp rate of 3.3 K/s presented in Fig. 1 (a) and (d). Fig. 4 exhibits the deconvolution of the TPD spectra of the Cab-O-Sil-M-7D sample with a ramp rate of 0.44 K/s and the Hi-Sil-233 sample with a ramp rate of 3.3 K/s into many separate desorption curves using the technique of iterative regression analysis. For a comparison with the above two techniques, values of E_d and ν corresponding to the first water TPD peaks are from 10 to 13 kcal/mol and from 5.3×10^4 to $6.7 \times 10^6 \text{ s}^{-1}$ for Cab-O-Sil-M-7D (mean values: 11.5 kcal/mol and $6.2 \times 10^5 \text{ s}^{-1}$) and from 9.5 to 11.5 kcal/mol and from 3.6×10^4 to $3.0 \times 10^5 \text{ s}^{-1}$ for Hi-Sil-233 (mean values: 10.5 kcal/mol and $1.4 \times 10^5 \text{ s}^{-1}$).⁸

Overall, values of E_d and ν for the first TPD peaks of Cab-O-Sil-M-7D and Hi-Sil-233 obtained from the iterative regression analysis technique are consistent with those obtained from the other two techniques. However, the agreement is much better between the iterative regression analysis and the variable linear ramp techniques than between the technique based on the plots of $\ln(-d\sigma/dt)$ vs. $1/T$ at the onset of the desorption and either

of the other techniques. But considering our limitation in extending the variable linear ramp technique to broader desorption peaks at high temperatures as mentioned above, iterative regression analysis is our technique of choice to extract detailed kinetic parameters from all TPD peaks.

Kinetic parameters of water desorption from Cab-O-Sil-M-7D and Hi-Sil-233:

The values of E_d and v for the different desorption curves for Cab-O-Sil-M-7D and Hi-Sil-233 are presented in the following tables II and III.

	Curve I	Curve II	Curve III	Curve IV	Curve V	Curve VI
n	1	1	2	2	2	2
E_d (kcal/mol) -variable linear ramp-	9-12	14.8-20.4 (assuming sharp peak)				
E_d (kcal/mol) -iterative regression analysis-	10.0-13.0	11.1-14.3	18.5-21.5	24.0-26.8	31.3-36.7	51.2-59.1
v (s ⁻¹) -variable linear ramp-	2.0 × 10 ³ - 7.3 × 10 ⁵	2.0 × 10 ⁴ -4.1 × 10 ⁶ (assuming sharp peak)				
v (s ⁻¹) -iterative regression analysis-	3.2 × 10 ⁴ - 3.2 × 10 ⁶	1.1 × 10 ³ - 2.9 × 10 ⁴	3.1 × 10 ⁵ - 3.7 × 10 ⁶	3.2 × 10 ⁶ - 9.4 × 10 ⁶	1.0 × 10 ⁷ - 1.0 × 10 ⁹	1.0 × 10 ¹¹ - 3.6 × 10 ¹³

Table II: The values of E_d and v for the different deconvoluted desorption curve of Cab-O-Sil-M-7D by the variable linear ramp and the iterative regression analysis techniques.

	Curve I	Curve II	Curve III	Curve IV
n	1	1	2	2
E_d (kcal/mol) -variable linear ramp-	9.5-14.5	19.6-28.9 (assuming sharp peak)		
E_d (kcal/mol) -iterative regression analysis-	9.5-11.5	13.4-14.3	22.9-26.7	30.1-35.7
v (s ⁻¹) -variable linear ramp-	1.1 × 10 ³ - 1.6 × 10 ⁸	3.0 × 10 ⁵ -8.7 × 10 ⁶ (assuming sharp peak)		
v (s ⁻¹) -iterative regression analysis-	3.6 × 10 ⁴ - 3.0 × 10 ⁵	1.4 × 10 ⁴ - 3.6 × 10 ⁴	5.1 × 10 ⁶ - 1.2 × 10 ⁸	8.3 × 10 ⁷ - 1.8 × 10 ⁹

Table III: The values of E_d and v for the different deconvoluted desorption curve of Hi-Sil-233 by the variable linear ramp and the iterative regression analysis techniques.

It is noted that the orders of reaction in the above tables are based on the assumption that the first desorption peak (<400 K) in each TPD spectrum is physisorbed in origin ($n = 1$). The second deconvoluted desorption curves (curve IIs) in each spectrum have $E_d < 16$ kcal/mol and are also classified to have $n = 1$. Other deconvoluted desorption curves are assumed to be chemisorbed in origin and assigned $n = 2$. This assignment is in agreement with recently publications of TPD data of water desorption from silica surfaces.^{6,7,9} In these publications, physisorbed water was reported to have activation energies in the range of 6-16 kcal/mol, while chemisorbed water (water molecules bonded to surface Si-OH and surface condensation of Si-OH) was reported to have activation energies in the range of 20 kcal/mol to > 50 kcal/mol. It can also be observed from tables II and III that ν tends to increase as E_d increases. This is in qualitative agreement with the results obtained for fumed silica (Aerosil A-3300) reported by Gun'ko et al.⁶ who cited values of ν starting from 10^6 s^{-1} for physisorbed water (with $E_d \sim 15$ kcal/mol) to between 10^9 - 10^{12} s^{-1} for chemisorbed water (with $E_d > 40$ kcal/mol). Chemisorbed water, which is formed by the condensation of hydroxyls (OH) from silanol groups (Si-OH) at the surface of silica, is expected to have a vibrational frequency closer to that of silica's surface phonons (10^8 - 10^{13} s^{-1}). H_2O molecules, which are bonded to OH groups, should have a smaller vibrational frequency due to the damping effect of the cushion layer of silanol groups (Si-OH). An illustration of the different bonding arrangements of water on silica's surface published by Feng et al.⁷ is presented in Fig. 5 of this report to help our visualization of the above mentioned damping effect. Physisorbed H_2O , for the same reason, is expected to have an even smaller vibrational frequency.

The evolution of H₂O coverage on the surface of Cab-O-Sil-M-7D and Hi-Sil-233

One question of practical importance in engineering is how the wt. % of water in these silica particles changes with time in vacuum at a given temperature. Assuming a good vacuum (ignoring the problem of water reabsorption from the environment) one may calculate the wt. % of H₂O retained on the silica surfaces as a function of time as following:

For n = 1

From equation (1), one can write:

$$-\frac{d\mathbf{s}}{\mathbf{s}} = (\mathbf{u} e^{-\frac{E_d}{RT}})dt$$

or

$$\ln \mathbf{s} = -(\mathbf{u} e^{-\frac{E_d}{RT}})t$$

$$\mathbf{s}(t) = \mathbf{s}_o e^{-(\mathbf{u} e^{-\frac{E_d}{RT}})t}$$

Since $\sigma_o = 1$, the wt. % of water retained on the silica surfaces after a time t is:

$$wt \% \text{ retained} = 100 \times \frac{\mathbf{s}(t)}{\mathbf{s}_o} = 100 \times e^{-(\mathbf{u} e^{-\frac{E_d}{RT}})t} \quad (11)$$

For n = 2

From equation (1), one can write:

$$-\frac{d\mathbf{s}}{\mathbf{s}^2} = \mathbf{u} \mathbf{s}^2 e^{-\frac{E_d}{RT}}$$

or

$$S(t) = \frac{S_o}{S_o \left(u e^{-\frac{E_d}{RT}} \right) t + 1}$$

Since $\sigma_o = 1$, the wt. % of water retained on the silica surfaces after a time t is:

$$Wt \% \text{ retained} = 100 \times \frac{1}{\left(u e^{-\frac{E_d}{RT}} \right) t + 1} \quad (12)$$

Based on the values of E_d and v from tables I & II and equations (11)-(12), the wt. % of water retained on the surface of silica kept in a good vacuum environment at a given temperature as a function of time can be predicted. Fig. 6 shows the plots of wt. % of water retained on the surfaces of silica vs. time at 300 K in a good vacuum environment when $E_d = 12$ kcal/mol and $u = 6.0 \times 10^5 \text{ s}^{-1}$ (a), when $E_d = 14.3$ kcal/mol and $u = 3.6 \times 10^4 \text{ s}^{-1}$ (b), when $E_d = 21.5$ kcal/mol and $u = 3.7 \times 10^6 \text{ s}^{-1}$ (c), when $E_d = 22.9$ kcal/mol and $u = 5.1 \times 10^6 \text{ s}^{-1}$ (d), when $E_d = 24$ kcal/mol and $u = 3.2 \times 10^6 \text{ s}^{-1}$ (e), and when $E_d = 26.8$ kcal/mol and $u = 9.4 \times 10^6 \text{ s}^{-1}$ (f). Fig. 7 shows the plot of wt. % of water retained on the surface of silica in a good vacuum environment when $E_d = 14.3$ kcal/mol, $u = 3.6 \times 10^4 \text{ s}^{-1}$, and $T = 320$ K (a); when $E_d = 21.5$ kcal/mol, $u = 3.7 \times 10^6 \text{ s}^{-1}$, and $T = 320$ K (b); when $E_d = 26.8$ kcal/mol, $u = 9.4 \times 10^6 \text{ s}^{-1}$, and $T = 320$ K (c); when $E_d = 31.3$ kcal/mol, $u = 2.0 \times 10^7 \text{ s}^{-1}$, and $T = 320$ K (d); when $E_d = 26.8$ kcal/mol, $u = 9.4 \times 10^6 \text{ s}^{-1}$, and $T = 500$ K (e); and when $E_d = 31.3$ kcal/mol, $u = 2.0 \times 10^7 \text{ s}^{-1}$, and $T = 500$ K (f).

It is seen that physisorbed water can be effectively pumped out at room temperature or at a slightly elevated temperature of 320 K in a matter of hours. Chemisorbed water with high activation energies of desorption (>30 kcal/mol) essentially will not escape the silica surfaces in 100 years even at 320 K, while a significant amount of the chemisorbed water

with medium activation energies (18.5-26.8 kcal/mol) will leave the silica surfaces in that time span. We also see that the outgassing due to water desorption from silica surfaces becomes much faster at 500 K than at 300K. This is not surprising since the temperature term goes exponentially in equations (11) and (12). It is clear from Fig. 7(e) that a good heat treatment to 500 K for many days would effectively eliminate the problem of water outgassing from the silica surfaces for the next 100 years, provided that the silica surfaces are not re-exposed again to moisture!

Weight percentages of water on as-received Cab-O-Sil-M-7D and Hi-Sil-233

First, the water signals detected at the mass spectrometer was converted to the number of water molecules per second striking a unit area of the entrance orifice of the mass spectrometer chamber through the use of a calibration curve. Since the Pt envelope containing silica powders was only 1-2 mm away from the entrance orifice of the mass spectrometer, it is reasonable to assume that the number of water molecules per second striking a unit area of the entrance orifice of the mass spectrometer chamber is the same as the number of water molecules per second leaving a unit surface area of the front side of the Pt envelope (which has holes poked all over its 1cm x 1cm surface area). The wt. % of water in the silica powder is simply the ratio of the weight of water desorbed and the weight of silica powders and can be obtained as following:

$$wt \% = \frac{\int_{t_o}^{t_{end}} \Gamma dt \times A \times \frac{M_{H_2O}}{N_{AV}}}{W_{silica}} \times 100 \quad (13)$$

where Γ is the detected H₂O desorption rate (molecules.cm⁻².s⁻¹), A is surface area of the Pt envelope facing the mass spectrometer (1cm x 1cm), M_{H₂O} is molecular weight of

water, N_{AV} is Avogadro number, w_{silica} is the weight of silica powders, and t_o and t_{end} are start time and end time of the desorption process. The weight percentages of water in Cab-O-Sil-M-7D and Hi-Sil-233 according to equation (13) are on the order of 0.38 wt. % and 0.67 wt. % respectively. To be more accurate, we have to take into account that the samples were pumped in the load-lock chamber for ~ 30-45 minutes prior to being introduced into the TPD main chamber. This is enough time to pump out roughly 85- 95 % of the most loosely bonded physisorbed water molecules from silica surfaces (first peaks in the TPD spectra), according to Fig. 6(a). In addition, the TPD spectrum for Cab-O-Sil-M-7D does not go down to background level at 800 K. The weight percentages of water reported here are, therefore, only rough estimates and serve as lower limits. The actual weight percentages of water on Cab-O-Sil-M-7D and Hi-Sil-233 are expected to be a factor of 2 or 3 higher than the numbers quoted above. However, the weight percentages of chemisorbed water are only roughly 0.25 and 0.44 for Cab-O-Sil-M-7D and Hi-Sil-233. Within the chemisorbed water, only ~ 60 % have activation energies of desorption in the range of 18.5 kcal/mol to 26.8 kcal/mol. This translate to 0.15 wt. % and 0.26 wt. % of chemisorbed water with activation energies < 27 kcal/mol for Cab-O-Sil-M-7D and Hi-Sil-233.

Comparison with water desorption data on M97 series silicones:

In M97 series silicones, Cab-O-Sil-M-7D fillers occupy ~ 21.6 wt. % and Hi-Sil -233 fillers occupy ~ 0.4 wt. %. Assuming that all the water outgassing from the silicones originates from silica fillers, the 0.38 wt. % and 0.67 wt. % of water from Cab-O-Sil-M-7D and Hi-Sil-233 translate into ~ 0.11wt. % (\times a factor of 2 or 3 to correct for the physisorbed water molecules that had been pumped out prior to taking TPD spectra) of

water in M97 series silicones. This number is within the range of 0.1 to 0.4 wt. % we reported earlier for M9787 silicone.¹ This agreement confirms our suggestion that adsorbed H₂O and Si-OH bonds on the silica surfaces are the major contributors to water outgassing from M97 series silicones. However, with decent pumping before vacuum packaging, only the chemisorbed water from the silica fillers' surfaces with activation energies < 27 kcal/mol (0.15 wt. % and 0.26 wt. % for Cab-O-Sil-M-7D and Hi-Sil-233, or 0.04 wt. % for silicones consisting 21.6 wt. % and 4 wt. % of Cab-O-Sil-M-7D and Hi-Sil-233) will contribute to long-term water outgassing.

The activation energy of desorption and pre-exponential factor for physisorbed water we reported for M9787 silicone are ~ 15 kcal/mol and $8.1 \times 10^5 \text{ s}^{-1}$. These are on the same order of magnitude with those measured for Cab-O-Sil-M-7D and Hi-Sil-233 in this report. The information on the kinetic parameters for chemisorbed water in this report is, however, expected to have much more details and to be more accurate than that reported earlier for M9787 silicone.¹ This is partly due to the inherent higher accuracy of the iterative regression analysis technique as mentioned above over the technique based on the Arrhenius plot of $\ln(-d\sigma/dt)$ vs. $1/T$, and partly because in the current experiments with silica we have been able to heat the sample from 300 to 850K (instead of from 300 to 500K for M9787), thus enabling more detailed deconvolution of the chemisorbed species.

IV. CONCLUSION

We performed temperature programmed desorption up to 850K on Cab-O-Sil-M-7D and Hi-Sil-233 silica particles. Our data show that the weight percents of water in the Cab-O-Sil-M-7D and Hi-Sil-233 silica particles were on the order of 0.38 (\times a factor of 2-3) and 0.67 (\times a factor of 2-3) respectively. It is interesting to note that the equivalent surface areas for Cab-O-Sil-M-7D and Hi-Sil-233 are 195 m²/g and 137 m²/g, respectively, but the weight % of water on Hi-Sil-233 is almost twice that of water on Cab-O-Sil-M-7D. In term of monolayers/cm², there are on the order of 0.14 monolayers/cm² (\times a factor of 2-3) and 0.34 monolayers/cm² (\times a factor of 2-3) of water on the surfaces of Cab-O-Sil-M-7D and Hi-Sil-233, respectively. If only chemisorbed water (from Si-OH bonds) is concerned, the numbers are \sim 0.055 monolayers/cm² and 0.132 monolayers/cm² of water for Cab-O-Sil-M-7D and Hi-Sil-233, respectively. If one assumes that it takes 2 Si-OH bonds to form one H₂O molecules, there are \sim 1.31×10^{13} Si-OH bonds/cm² and 3.14×10^{13} Si-OH bonds/cm² on the surfaces of Cab-O-Sil-M-7D and Hi-Sil-233, respectively. Physisorbed water molecules in both types of silica had activation energies of 9-14.5 kcal/mol. The activation energies of desorption for chemisorbed water could be from 18.5 kcal/mol to 59.1 kcal/mol for Cab-O-Sil-M-7D and from 22.9 kcal/mol to 36.7 kcal/mol for Hi-Sil-233. Our calculation suggests that physisorbed water can be effectively pumped away at room temperature (preferably at 320 K) in a matter of hours. Chemisorbed water with high activation energies of desorption (>30 kcal/mol) will not escape the silica surfaces in 100 years, while a significant amount of the chemisorbed water with medium activation energies (18.5-26.8 kcal/mol) will leave the silica surfaces in that time span. Most of the chemisorbed water with activation energies < 30 kcal/mol can be pumped away in a matter of days in a good vacuum environment at an elevated temperature of 500

K. We had previously measured about 0.1 to 0.4 wt. % of water in M9787 silicones. Our current data show that silicones consisting of 21.6 wt. % Cab-O-Sil-M-7D and 4 wt. % Hi-Sil-233 silica particles would have on the order of 0.11 (\times a factor of 2 to 3) wt. % of water. And within this 0.11 (\times a factor of 2 to 3) wt. % of water, only 0.04 wt. % is due to chemisorbed water with activation energies of desorption < 27 kcal/mol. We conclude that absorbed H_2O and Si-OH bonds on the silica surfaces are the major contributors to water outgassing from M97 series silicones.

V. ACKNOWLEDGEMENT

This work was performed under the auspices of the U.S. Department of Energy by Lawrence Livermore National Laboratory under contract No. W-7405-ENG-48.

REFERENCES

1. L. N. Dinh, M. Balooch, J. D. LeMay, Desorption kinetics of H₂O, H₂, CO, and CO₂ from silica reinforced polysiloxane, UCRL-ID-135387, Lawrence Livermore National Laboratory.
2. K. H. Van Heek and H. Juntgen, Berichte Der Deutschen Bunsengesellschaft Fur Physikalische Chemie, vol. **72**, 1223(1968).
3. J. B. Miller, H. R. Siddiqui, S. M. Gates, J. N. Russel, jr., J. T. Yates, jr., J. Chem. Phys. **87**, 6725 (1987).
4. We also monitored the desorption of masses: 2, 28, and 44. Similar to the results reported in reference 1 above, the integrated H₂O signal is about 2 decades stronger than the combined signals from H₂, CO, and CO₂.
5. These spectra have been background subtracted from an essentially flat response of the Pt foil envelope.
6. V. M. Gun'ko et al., Journal of Mass Spectrometry and Ion Processes **172**, 161 (1998).
7. A. Feng et al., Journal of Colloid and Interface Science **180**, 276 (1996).
8. The curve fitting statistics here were obtained from the Chi-square method (χ^2).
9. O. Sneh, M. A. Cameron, S. M. Goerge, Surf. Sci. **364**, 61 (1996).

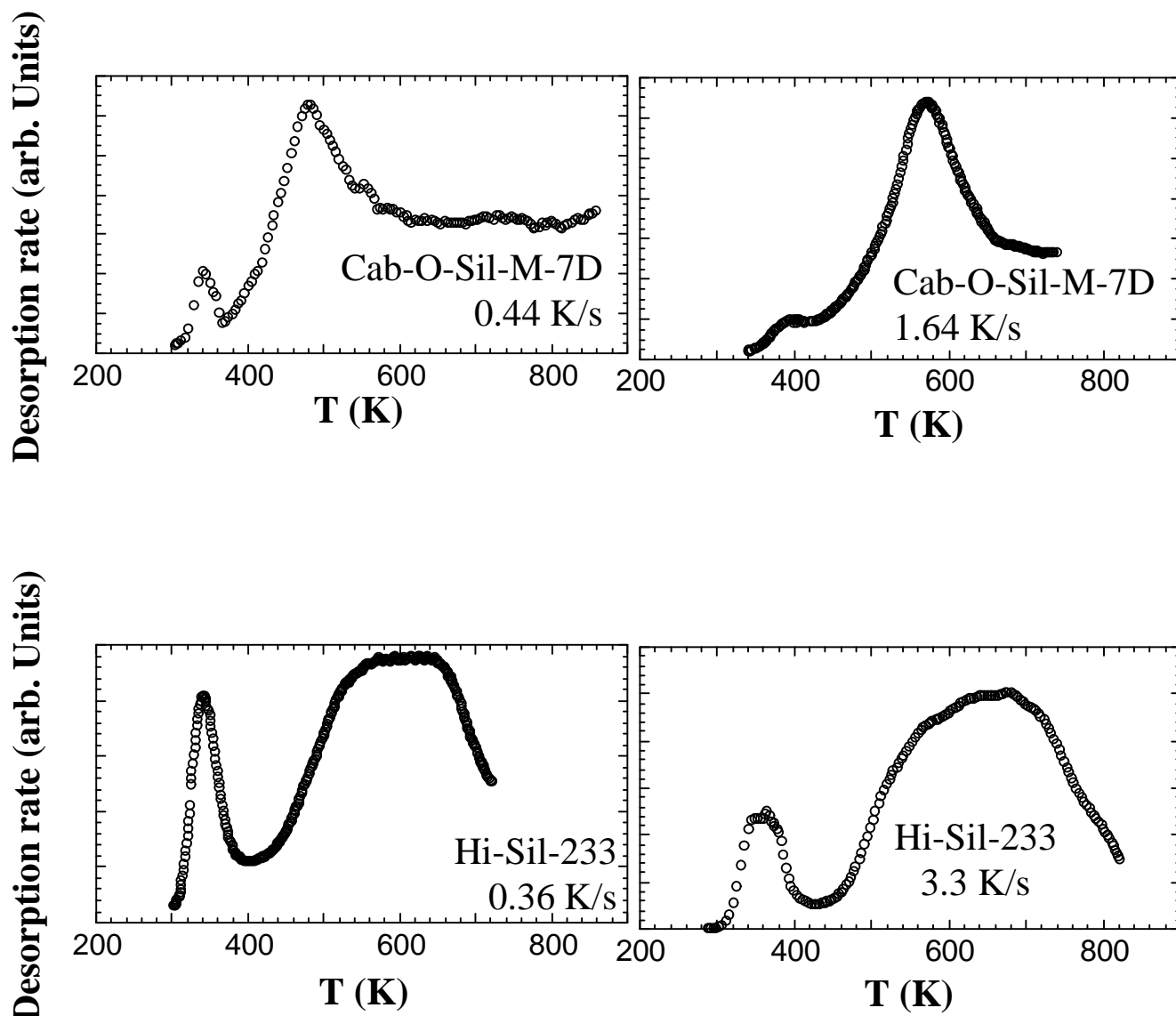


Fig. 1: H₂O TPD spectra from Cab-O-Sil-M-7D and Hi-Sil-233.

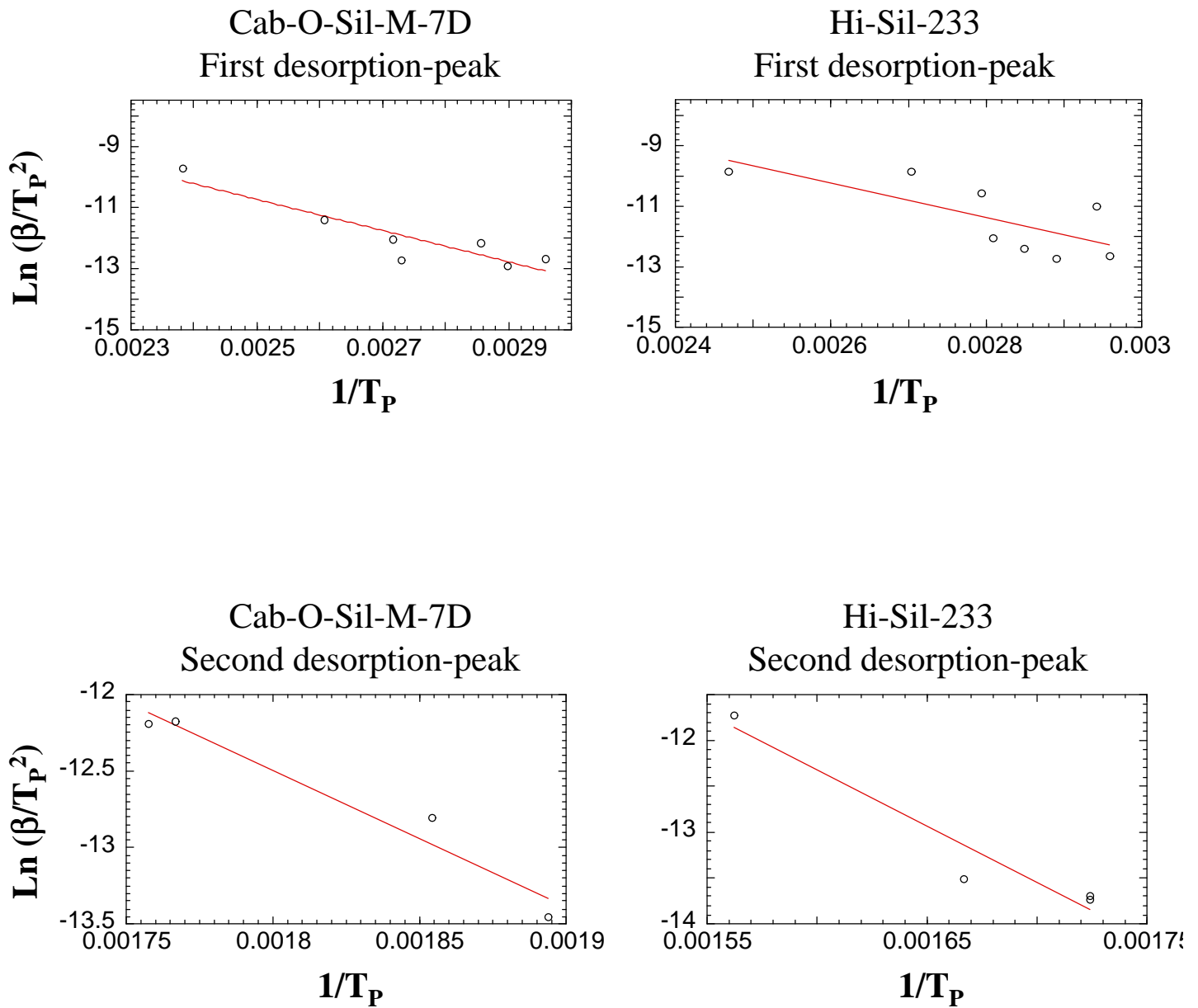


Fig. 2: Plots of $\ln(\beta/T_p^2)$ vs. $1/T_p$ for the first and second TPD peaks of Cab-O-Sil-M-7D and Hi-Sil-233.

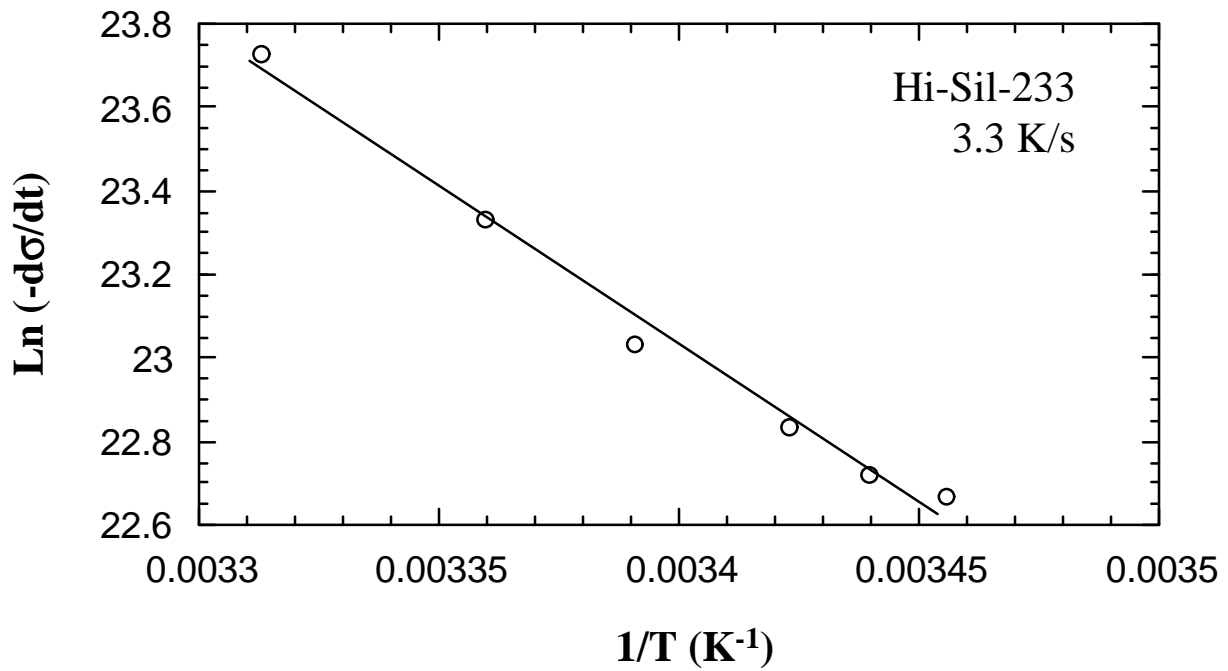
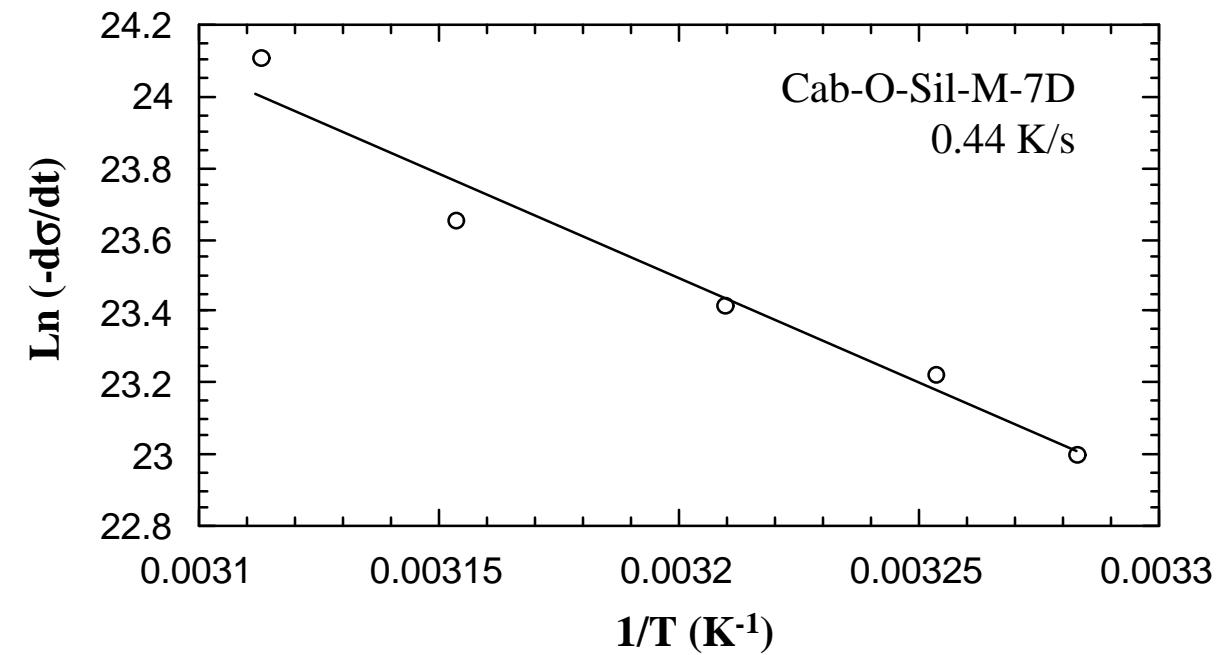


Fig. 3: $\ln(-d\sigma/dt)$ vs. $1/T$ at the onset of the desorption for the first desorption peak from Cab-O-Sil-M-7D and Hi-Sil-233.

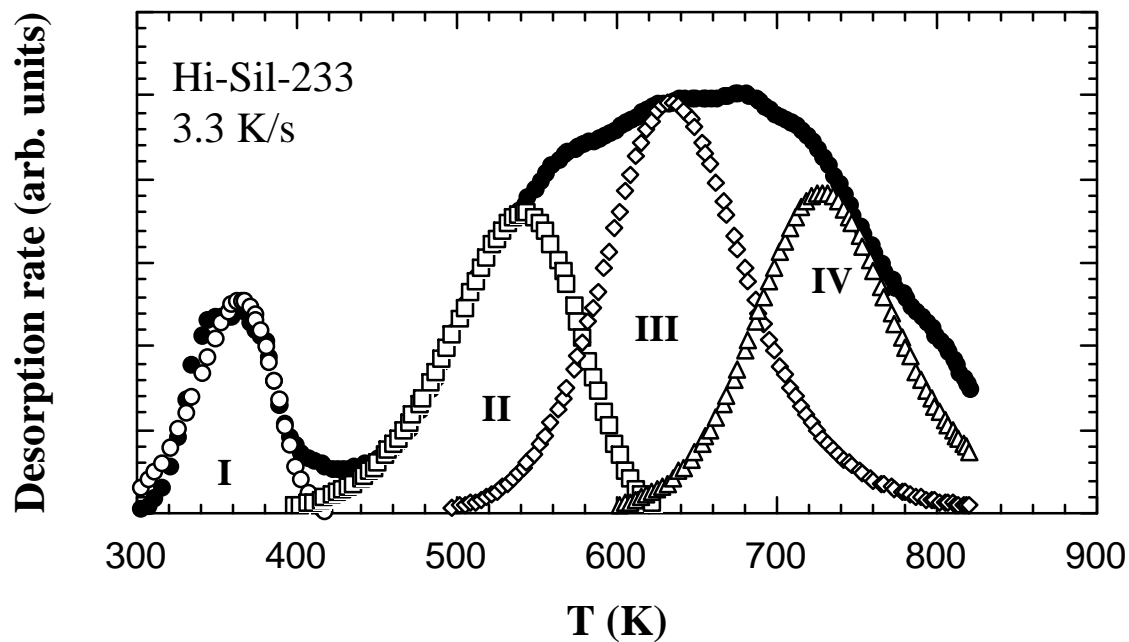
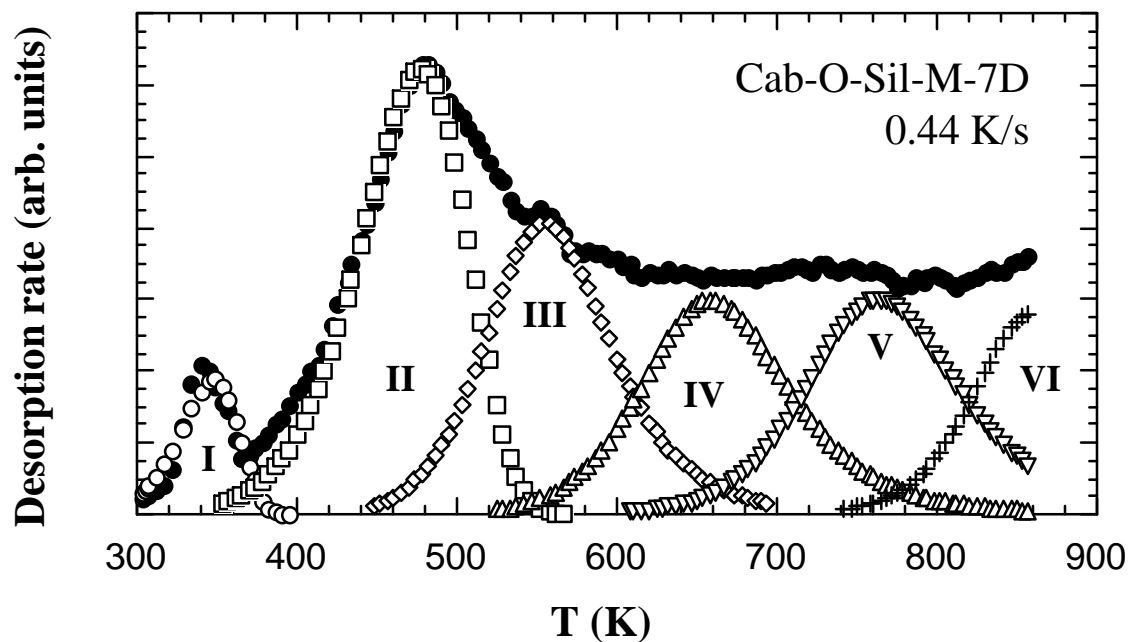


Fig. 4: The deconvolution of the TPD spectra of Cab-O-Sil-M-7D and Hi-Sil-233 into many separate desorption curves using the technique of iterative regression analysis.

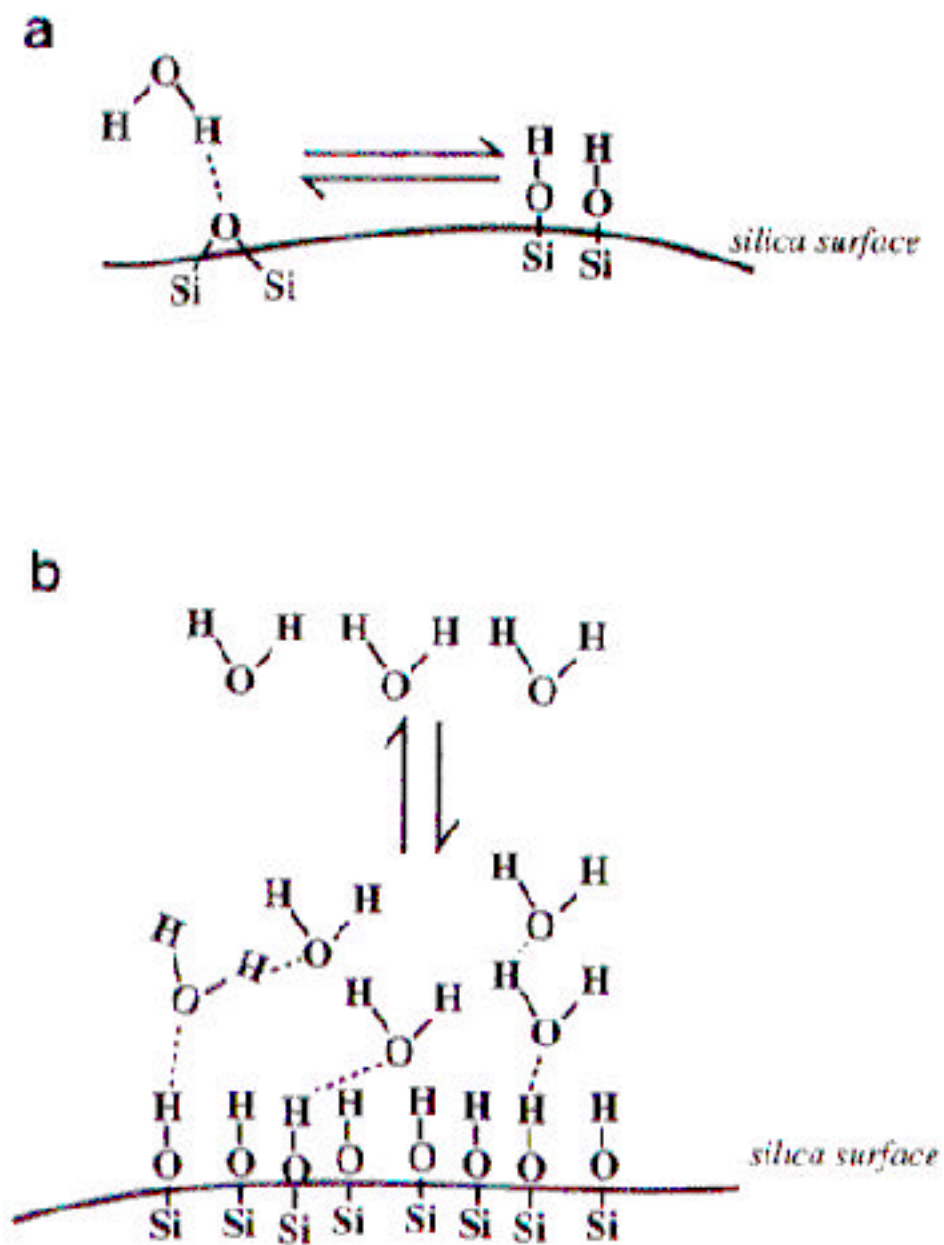


Fig. 5: An illustration of the different bonding arrangements of water on silica's surface published by Feng et al..

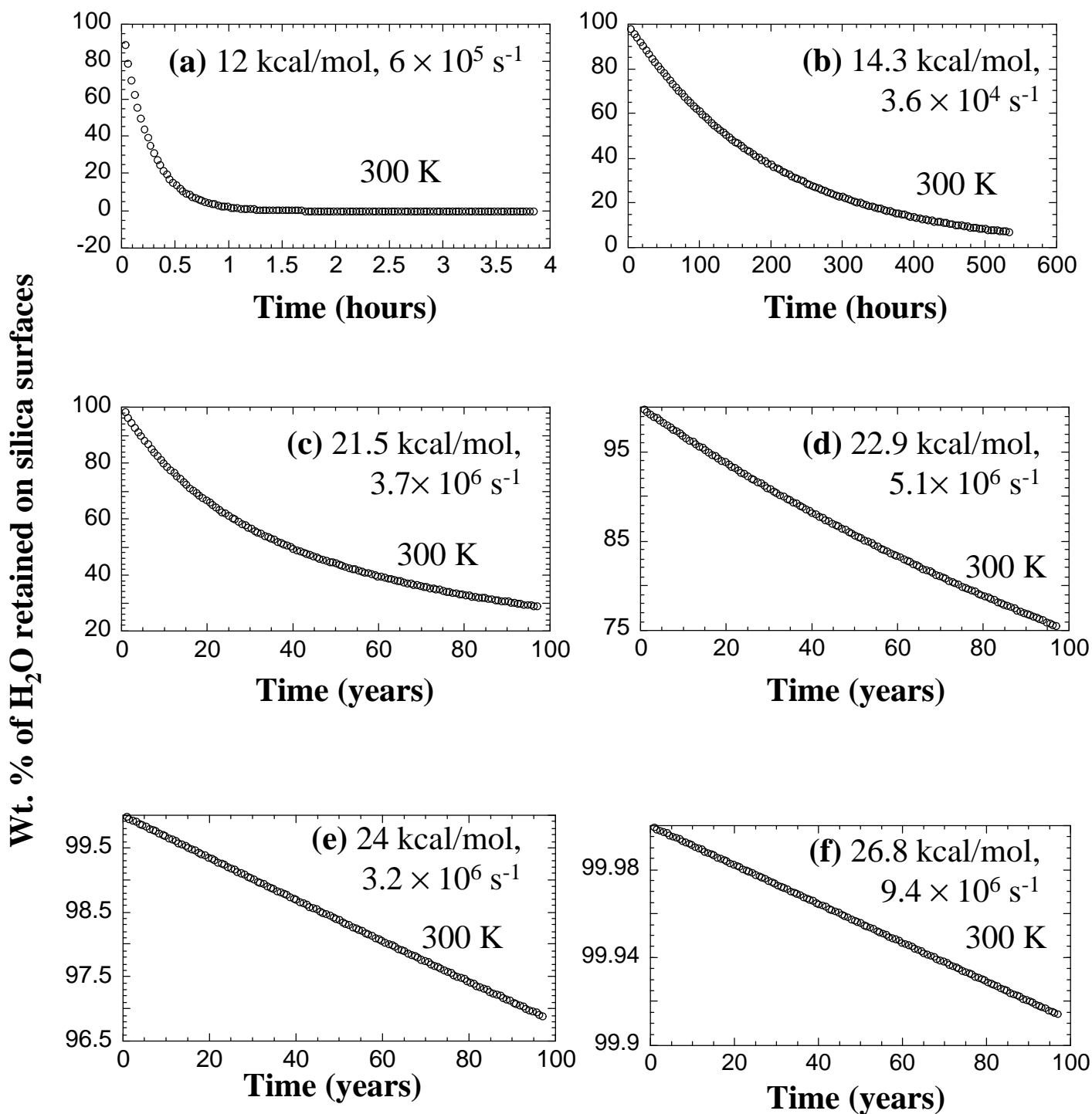


Fig. 6: Wt % of water retained on the surfaces of silica vs. time at 300 K in a good vacuum environment.

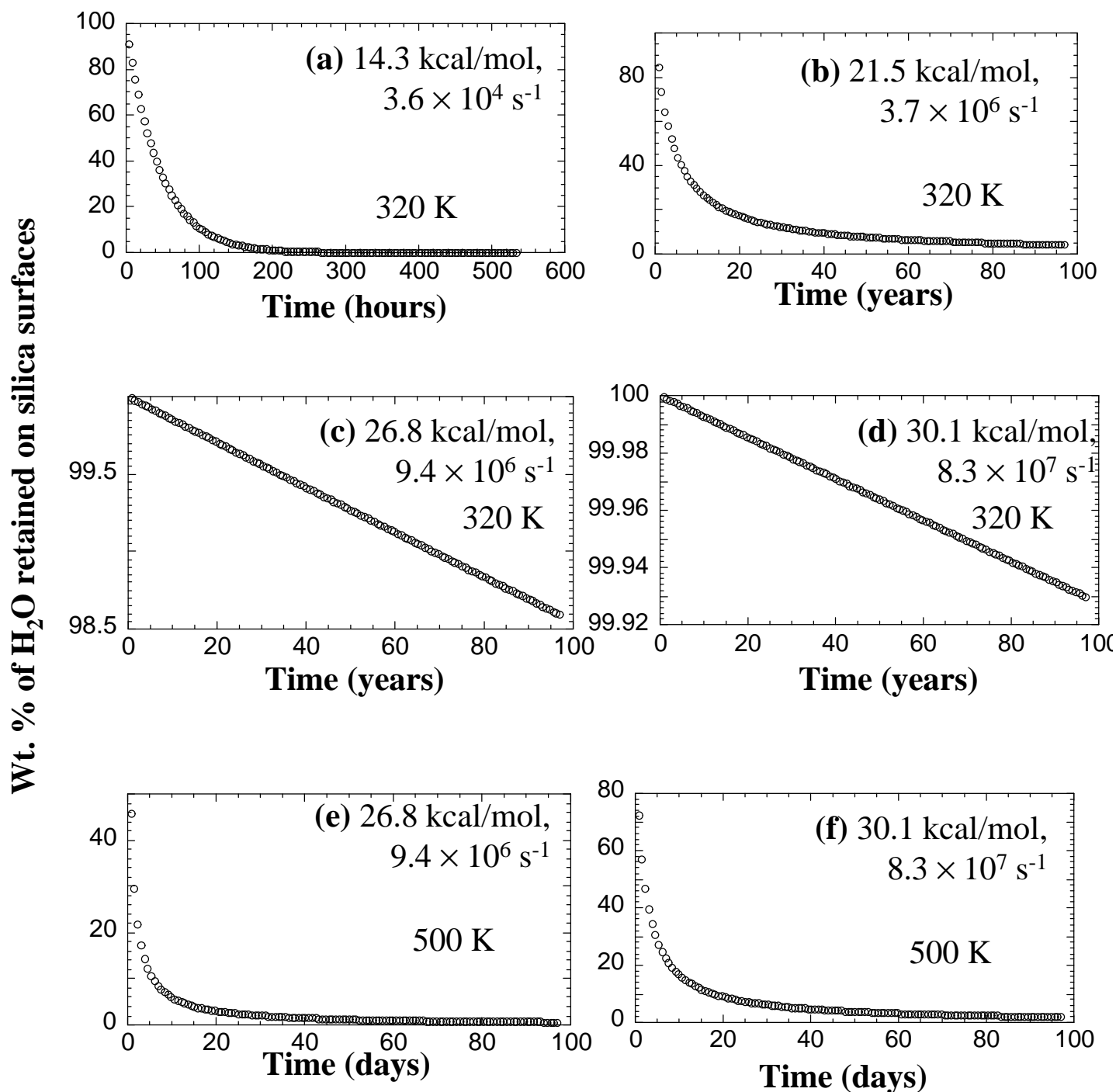


Fig. 7: Wt % of water retained on the surfaces of silica vs. time at 320 K and 500 K in a good vacuum environment.